Title: MiR-124 contributes to M2 polarization of microglia and confers brain inflammatory protection via the C/EBP-α pathway in intracerebral hemorrhage

Author: Anyong Yu Tianxi Zhang Haizhen Duan Yong Pan Xiaojun Zhang Guang Yang Juan Wang Yi Deng Zhao Yang

PII: S0165-2478(16)30345-5
DOI: http://dx.doi.org/doi:10.1016/j.imlet.2016.12.003
Reference: IMLET 5963

To appear in: *Immunology Letters*

Received date: 27-9-2016
Revised date: 16-12-2016
Accepted date: 22-12-2016

Please cite this article as: Yu Anyong, Zhang Tianxi, Duan Haizhen, Pan Yong, Zhang Xiaojun, Yang Guang, Wang Juan, Deng Yi, Yang Zhao.MiR-124 contributes to M2 polarization of microglia and confers brain inflammatory protection via the C/EBP-α pathway in intracerebral hemorrhage.*Immunology Letters* http://dx.doi.org/10.1016/j.imlet.2016.12.003

MiR-124 contributes to M2 polarization of microglia and confers brain inflammatory protection via the C/EBP-α pathway in intracerebral hemorrhage

Anyong Yu [b,1], Tianxi Zhang [b,1], Haizhen Duan [b], Yong Pan [b], Xiaojun Zhang [b], Guang Yang [b], Juan Wang [a], Yi Deng [a], Zhao Yang [a,*]

a. Department of Neurology, Yongchuan Hospital, Chongqing Medical University, Chongqing 402160, China

b. Department of Emergency, The First Affiliated Hospital of Zunyi Medical College, Guizhou 563003, China

1. Theses authors contributed equally to this study.

*Corresponding author.

Email: yangzhao5140@sohu.com

Tel: +86-23-85381660; Fax: +86-23-85381660;

Highlights

>miR-124 was significantly increased in M2-polarized microglia. >Transfection of miR-124 mimics decreased proinflammatory cytokine secretion. >miR-124 decreased brain levels of C/EBP-α and significantly reduced brain injury in ICH mice.

Abstract

Microglia mediated inflammation contributes to intracerebral hemorrhage (ICH) induced secondary injury. Activated microglia has dual functions as pro-inflammatory (M1) and anti-inflammatory (M2) factors in brain injury and repair. MiR-124 is a potent anti-inflammatory agent which affects microglia after brain injury. However, the potential of modulating the M1/M2 polarization of microglia after ICH has not been reported. In this experiment, we detected the effect of miR-124 on the M1/M2 polarization state. In addition, the ability miR-124 to subsequently impacted neurological deficit and cerebral water content of ICH mice were studied. Furthermore, the relationship between miR-124 and C/EBP-α target was detected. We found that miR-124 significantly increased in M2-polarized microglia. Transduction of miR-124 mimics decreased proinflammatory cytokine levels. A coculture model of microglia and neuron indicated that M2-polarized microglia protected neuron damage. Furthermore, miR-124 banded to the 3-untranslated region of C/EBP-α and downregulated its protein levels. In vivo, infusion of miR-124 decreased brain levels of C/EBP-α and significantly reduced brain injury in ICH mice. Thus, miR-124 ameliorated ICH-induced inflammatory injury by modulating microglia polarization toward the M2 phenotype via C/EBP-α. MiR-124 regulatory mechanisms also might represent new therapeutic strategy in ICH.

Keywords: miR-124; M2 polarization; microglia; inflammation; C/EBP-α; ICH

Introduction

Intracerebral hemorrhage (ICH) is a serious problem to people's health and quality of life, and accounts for 10%-15% of strokes[1-3]. Although people took the treatment such as hemostatic, dehydration, and surgery, the neurofunction after ICH is still difficult to recover[4-6]. Numerous studies demonstrate that inflammation mediated secondary injury contributes to neuro-defect after intracerebral hemorrhage. Inflammation associated signals cause microglia activation, permeability of the endothelial cells, and release of inflammatory mediators, leading to neuron death and brain damage[7-9].

Microglia is one of the inflammatory cells in the central nervous system (CNS). Microglia in the central nervous system plays a diverse role through different polarization. Related evidence suggest that microglia polarizes into two main states, namely classically activated M1 and alternatively activated M2[10-12]. Classical M1 activation is related with proinflammatory molecule induction, while alternative M2 activation is associated with neuroprotective roles[13-15].

MiRNAs are important non-coding small RNAs, modulate gene expression through the transcription regulation function, involving the life stages of growth, development and death[16-18]. It has been found that miRNAs could regulate the gene transcription and their associated signaling pathway expression level, which involved in polarization of microglia[19-21]. Related evidence showed that miR-124, the most abundant microRNA in the brain, could not only regulate neuron differentiation and microglia development, but also polarize macrophages and microglia towards the M2 phenotype in ischemic stroke and experimental autoimmune encephalomyelitis (EAE) models[21-23].

However, the exact mechanism of miR-124 to regulate M1/M2

polarization in ICH has not been identified. In the current study, we detect the miR-124 levels, and further explore the potential role in ICH. We expect miR-124 may provide new insights into the understanding of cerebral protection and act as a neuroprotective agent for ICH therapeutics.

Materials and Methods

Primary Cell Cultures

Cortical neuronal were prepared from embryonic day 16-18 C57BL/6 mice. Briefly, the cerebral cortices and hippocampus of fetus mice were dissected out and the meninges were carefully removed. Cells (1×10^6 cells/mL) were maintained in poly-D-lysine (Sigma, St. Louis, MO) coated plates in Dulbecco's modified eagle medium (DMEM) medium (Life Technologies) with 10% fetal bovine serum (FBS) (Life Technologies). After 4-6 h of culture, the cultures were replenished with Neurobasal medium (Life Technologies) containing 100 U/mL penicillin, 100 μg/mL streptomycin, 2% B27, and 0.5 mM glutamine (Life Technologies) at 37°C with 5% CO_2. The medium was changed every three days. For primary microglia cells, glial cells were isolated from the brains of rat pups and were placed in a 75 cm2 flask at a density of 1×10^6 cells/ml of DMEM (Sigma-Aldrich) supplemented with 20% fetal bovine serum (FBS) and 1% antibiotic antimycotic solution (Sigma-Aldrich). The flasks were then placed in a humidified atmosphere containing 5% CO_2 and 95% air at 37°C. The culture medium was changed every 48 to 72 hours. Microglia was isolated from the mixed glial population when mixed glial cells were confluent (12 to 14 days). The purity of microglia was assessed by immunofluorescence. Microglial cultures with more than 98% purity were used for the study.

Animals

Male C57BL/6 mice (8-10 weeks) were purchased from the Animal institute of Chongqing Medical University and bred under specific pathogen-free conditions. Experiments were finished according to animal care guidelines approved by the Animal Ethics Committee of Chongqing Medical University. All experiments were performed and reported according to the Guide for the Care and Use of Laboratory Animals, 8th edition (2011) and the ARRIVE guidelines (http://www.nc3rs.org.uk /arriveguidelines).

Preparation of erythrocyte lysates

Blood were removed from C57BL/6 mice. Single-cell suspensions of erythrocytes were prepared. And then, 1×10^5 erythrocytes were incubated with 1 ml red blood cell lysing solution for 20 min, and centrifuged at 2000 rpm for 10 min. The supernatants were utilized as erythrocyte lysates.

Cell treatment

Microglia collected from culture flasks were seeded at a density of 3×10^5cells/well onto 24-well tissue culture plates. Microglia was stimulated with 10 μl erythrocyte lysates or PBS. After 3 days, culture supernatants were removed and further assessed for cytokine levels with qRT-PCR and ELISA assays. Cortical neurons were cultured in a 96-well plate with 1×10^4 cells per well. For the toxicity experiments, neuron was cultured for 4 h and then treated with microglia-conditioned medium. In addition, neurons were treated for 48 h for MTT and apoptosis assays.

Real-time PCR

Frozen mice brains were homogenized, and total RNA was obtained from

about 4×4×4 mm^3 volume of perihematomal tissues at 3 days post-ICH using Trizol reagent (Invitrogen, Carlsbad, CA, USA) in compliance with the manufacture's instruction. The concentration of RNA was tested by a spectrophotometer. The M-MLV Reverse Transcriptase System (Promega, Madison, WI, USA) was performed for reverse transcription. The cDNA was stored at -20°C. Quantitative real-time PCR was fulfilled with a Light Cycler (Roche Diagnostics, Mannheim, GM) and with SYBR Green I in SYBR RT-PCR Kit (TaKaRa Biotechnology, Dalian, China) so as to enlarge and detect the mRNA expression. The transcript amount of the β-actin house keeping gene was quantified as an internal RNA control. Primers were purchased from BioAsia Corp. (Shanghai, China). The iNOS forward: 5'-GCCACCAACAATGGCAACA-3' and reverse: 5'-CGTACCGGATGAGCTGTGAATT-3'; The TNF-α forward: 5'-CA CGC TCT TC TG TCT ACTGA A C-3' and reverse: 5'- AT CT GAG TG TGA GG G T C T GG-3'. The IL-1β forward: 5'-CAG GCAA CCA CT TA CC TATTTA-3' and reverse: 5'-CCATA CAC ACGGACAA CAA CTA GA T -3'; The IL-10 forward: 5'-CGAC TGT TG CCT CT CG TACA-3' and reverse: 5'-AGGAGGTTCACAGCCCTTTT-3'; The Arg-1 forward: 5'-CGCCTTTCTCAAAAGGACAG-3' and reverse: 5'- CCAGCTCTT CATTGGCTTTC-3'; β-actin forward: 5'-GG CATCGTGATGGACTC CG-3' and reverse: 5'-GCTGGAAGGTGGACAGCGA -3'; miR-124 was detected using the miRNA RT kit (ABI) and TaqMan Universal PCR Master Mix (ABI) according to the manufacturer's instructions. U6 was used as an internal control. The relative quantification value for each target gene was performed using the comparative cycle threshold method. Experiments were carried out in triplicate for each data point. A threshold cycle value (CT) was calculated by the $^{\Delta\Delta}$CT method. The data were analyzed by using Light

Cycler Software 4.0 (Roche Diagnostics).

Western blot analysis

Briefly, proteins were separated from perihematoma tissues (80 mg) by SDS polyacrylamide gel electrophoresis and transferred onto polyvinylidene fluoride (PVDF) membranes (Amersham Pharmacia). The PVDF membranes were incubated with the primary antibodies, including: rabbit anti-mouse iNOS, TNF-α, IL-1β, IL-10 and Arg-1, followed by incubation with peroxidase-conjugated secondary antibodies (1:2000, Jingmei, China). The signals were detected with an ECL system (Amersham Pharmacia). The same membranes were probed with antibody for glyceradehyde-3-phosphate dehydrogenase (GAPDH) after being washed with stripping buffer. The signals were quantified by scanning densitometry and computer-assisted image analysates.

Cytotoxicity assay

The cytotoxic activity of microglia was measured by a 6 h lactate dehydrogenase release assay using CytoTox96 Non-radioactive Cytotoxicity Assay kit (Promega, Charbonnie'res-les-Bains, France) on 5×10^3 neuron/well. Neuron was then added to the wells with 2×10^3 microglia. Experiments were performed in quadruplet and the percentage of lysis was determined by OD490 measurement as described in the manufacturer's instructions. The percentage of cell mediated cytotoxicity was calculated according to the equation: % Specific Lysis = (effector /target cell mix LDH release-spontaneous effector LDH release)/ (maximum target LDH release - spontaneous target LDH release) ×100%:

MTT assay

Cell viability of neurone was assessed using 3-(4,5-dimethyl-2-thiazolyl)-2,5-diphenyl-2H-tetrazolium bromide (MTT, Sigma-Aldrich) assay. After 48 h, MTT (20 μL, 5 mg/ml) was added to the cells and incubated at 37°C for 4 h. A 150 μL aliquot of dimethyl sulfoxide was added and incubated for 10 min to dissolve the dark blue crystals. The absorbance was subsequently measured at 490 nm on a microplate reader (Multiskan MK3, Thermo Scientific, USA). The mean of readings of triplicate wells was taken as one value. The OD value for the control cultures was considered as 100% viability and viability in other samples is expressed as a percentage of viability in the control cultures.

Annexin-V-FLUOS apoptosis assay

Cells were collected and detected using the Annexin-V-FLUOS staining kit (Roche Applied Science). Briefly, cells were suspended in 500 μL of binding buffer and incubated at room temperature in the dark for 15 min after labeled with 5 μL of Annexin-V-fluorescein isothiocyanate (FITC) and 5 μL of propidium iodide. The stained cells were then visualized under a fluorescence microscope (Nikon, Eclipse E600). The cell apoptosis rate was calculated as the following formula: apoptosis rate = (apoptotic cell number/total cell number) × 100%.

TUNEL staining

The animals were deeply anesthetized and perfused through the ascending aorta with cold PBS followed by 4% paraformaldehyde, and the brains were

sectioned coronally into 20-mm-thick frozen slices. TUNEL staining was performed using an in situ cell death detection kit (Roche, Indianapolis, IN). The stained sections were photographed with a confocal fluorescence microscope (Leica, Wetzlar, Germany). The nuclei were stained with DAPI (blue), and the apoptotic cells were TUNEL positive (red). We calculated the number of DAPI positive cells (blue) and TUNEL positive cells (red). The percentage of TUNEL positive cells was calculated using the formula green/blue × 100%. Four quadrants were selected from each section, and the number of positive cells in each quadrant was counted. The average value was then calculated.

Oligonucleotide transfection

The miRNA mimics and the small interfering RNAs (siRNAs) were designed for not homologous to any mouse gene sequences. The siRNAs were designed by targeting mouse C/EBP-α transcripts. Oligonucleotide transduction was utilized with commercial reagents (Lipofectamine 2000.). Each transduction used 50 nmol/l of RNA duplexes.

Vector construction and luciferase reporter assays

To construct the miR-124 expression vector, the miR-124 gene was amplified from mouse genomic DNA and cloned into the pcDNA3.0 vector (Invitrogen Corp.). The luciferase complexes were designed by ligating oligonucleotides including the wild-type or mutated putative target site of the mouse C/EBP-α 3′-untranslated region (UTR) into the multi-cloning site of the p-MIR luciferase reporter vector (Ambion Inc., Austin, TX, USA). Microglia were cotransfected with 80 ng of the luciferase reporter plasmid, 40 ng of the pRL-TKRenilla-luciferase plasmid (Promega Corp., Madison,

WI, USA), and the indicated RNAs (final concentration 20 nmol/l). At 24 h, after the transduction, the firefly and Renilla luciferase activities were detected (Dual-Luciferase Reporter Assay; Promega Corp.). Each transduction was repeated twice.

ICH model

The ICH mice model was constructed according to previous report[24]. Mice (n=10 per group) were anesthetized with 10% chloralhydrate (350 mg/kg) and were placed in a stereotaxic frame (Alcott Biotech, Shanghai, China). Through a hole drilled in the skull, a 32-gauge needle was implanted into the caudate nucleus, 2.0 mm lateral to the midline, 1.0 mm anterior to the coronal suture and at a depth of 4.0 mm from the surface of the brain. Each mouse was microinjected with 20 μl of autologous whole blood (right striatum) taken from the tail vein over 10 min using a microinfusion pump (ALC-IP600, Alcott Biotech). Then the needle was pulled out without blood reflux after 5 min dwelling and the wound was sutured. Only the mouse observed neurological deficit was regarded as a successful model. The mice in sham operation group had the same operation but no blood was injected.

Intracerebroventricular injection

The in vivo transfection was performed according to the method described as follows: the stereotaxic coordinates were 0.5 mm posterior and 1.0 mm lateral to bregma and 2.5-3.0 mm ventral to the surface of the skull. The miR-124 mimics or miR-124 inhibitor (2 μg/2 μl) were added to 1.25 μl of Entranster™ in vivo transfection reagent. The solution was mixed gently, left for 15 min and then injected intracerebroventricularly (i.c.v.) using a micro syringe (Hamilton, NV, USA) under the guidance of the stereotaxic

instrument (RWD Life Science).

Neurological deficit scores

The neurological deficit were determined by neurological severity scores, a composite of motor, sensory, reflex, and balance tests according to previous report[25]. Neurological deficits were assessed 3 days after ICH using a 18-point neurological deficit scale, including neurological severity scores, a composite of motor, sensory, reflex, and balance tests. Scoring was performed by 2 trained investigators who were blind to animal grouping, and the mean score of the subscales was the final score of each mouse.

Brain water content

The extent of brain edema after ICH was determined by brain water content measurement on day 3 after ICH. The brains were removed and dissected into ipsilateral and contralateral striatum and cerebellum (which served as an internal control). The percentage of brain water content was calculated as (wet weight − dry weight)/wet weight × 100%

Statistical analysis

Data are represented as means ± standard errors of the means. Statistical analysis were performed using one-way analysis of variance (ANOVA) followed by Bonferroni's multiple comparison test. Differences were determined by using the Student two-tailed *t* test when two groups were compared.

Results

MiR-124 expression was downregulated in perihematoma tissue of ICH mice and erythrocyte lysates-treated microglia

To detect miR-124 expression, we utilized experimental ICH model and erythrocyte lysates-treated microglia model to measure miR-124 levels in vivo and in vitro. MiR-124 levels of perihematoma tissue or microglia were measured by real-time PCR at different time point after ICH or erythrocyte lysates treatment. We fount that the levels of miR-124 in perihematoma tissue of ICH were much lower than that in sham group (Fig.1A). We also used a cell culture model of ICH, erythrocyte lysates treatment to validate the specific change of miR-124 level. We found that the level of miR-124 in erythrocyte lysates treated microglia was much lower than that in PBS treated group at different time point in observation (Fig.1B) .

MiR-124 enhanced microglia M2 polarization in vivo and in vitro

To further investigate the role of miR-124 on microglia M1/M2 polarization in vivo, we analyzed M1/M2 markers in the perihaematomal region of cerebral tissues with qRT-PCR and western blot assays. Intracerebroventricular injection of miR-124 mimics or inhibitors was performed to upregulate or knockdown miR-124 in brain. We found that miR-124 mimics significantly decreased of M1 marker IL-1β, and TNF-α levels compared with those of miR-124 inhibitors group. In addition, miR-124 mimics significantly increased M2 marker IL-10 and Arg-1 levels compared with those of miR-124 inhibitors group (Fig.2). To detect the role of miR-124 on microglia M1/M2 polarization in vitro, we analyzed M1/M2 markers in erythrocyte lysates treated microglia with qRT-PCR and western blot assays. We also found that miR-124 attenuated M1 marker expressions and promoted M2 marker expressions in vitro (data not shown).

MiR-124 attenuated inflammatory damage in vivo and in vitro

To determine the contribution of miR-124 to neurological function, i.c.v. injection of miR-124 mimics or inhibitors were administered 10 min after ICH. Water content in mice brains and neurological injury were observed 3 days after ICH. We found that miR-124 mimics significantly reduced water content and neurological injury. On the contrary, miR-124 inhibitors significantly promoted water content and neurological injury (Fig. 3A and B). In addition, to explore whether miR-124 could inhibit toxicity of activated microglia to neuron in vitro, we also used an MTT assay to examine the effect of miR-124 on microglial toxicity to neuron. We found that miR-124 mimics significantly reduced microglial toxicity to neuron. On the contrary, miR-124 inhibitors significantly promoted microglial toxicity to neuron (Fig. 3C).

MiR-124 attenuated neuron apoptosis via Bcl-2/Bcl-xl pathway

ICH induced neuron apoptosis plays a vital role in inflammatory injury. We utilized TUNEL staining to analyze neuron apoptosis in the perihaematomal region of cerebral tissues 3 days after ICH. The results demonstrated that miR-124 mimics significantly reduced the numbers of TUNEL positive cells in the perihaematomal region. On the contrary, miR-124 inhibitors significantly promoted the numbers of TUNEL positive cells in the perihaematomal region (Fig. 4A). In addition, Bcl-2 and Bcl-xl are important factors for cell survival owing to antiapoptotic effects. We also examined the effect of miR-124 treatment on the Bcl-2 and Bcl-xl levels in the perihaematomal region. The results demonstrated that miR-124 mimics significantly increased Bcl-2/Bcl-xl expression in the perihaematomal region.

On the contrary, miR-124 inhibitors had the opposite results (Fig. 4B-C). Furthermore, we used flow cytometry assay to examine whether miR-124 could inhibit neuron apoptosis via Bcl-2/Bcl-xl pathway in vitro. The results demonstrated that miR-124 mimics significantly decreased neuron apoptosis ratio. On the contrary, miR-124 inhibitors significantly increased neuron apoptosis ratio via Bcl-2/Bcl-xl pathway in vitro (Fig. 4D-F).

C/EBP-α was a direct target of miR-124 in microglia

The 3′-UTR of C/EBP-α mRNA contains a putative miR-124 target sequence according to the target prediction program TargetScan (www.targetscan.org) (Fig.5A). To prove C/EBP-α was a direct target of miR-124 in microglia, we detected this relationship by a Dual-Luciferase reporter system. We found that co-expression with miR-124 mimics significantly suppressed the activity of a firefly luciferase reporter containing wild-type C/EBP-α 3′-UTR, while the phenomenon did not been detected on a reporter with a mutated C/EBP-α 3′ -UTR (Fig.5B). These results indicated that miR-124 likely attenuated C/EBP-α expression by directly binding target sites in the C/EBP-α 3′-UTR.

MiR-124 regulated C/EBP-α expression in vivo and in vitro

To analyze the role of miR-124 mimics or miR-124 inhibitors on the expression of miR-124, we found that transduction of miR-124 mimics improved miR-124 mRNA expression, while transduction of miR-124 inhibitors attenuated miR-124 mRNA expression (Fig. 5C). In addition, to identify whether miR-124 could inhibit C/EBP-α expression in vivo, we analyzed C/EBP-α expression in the perihaematomal region of cerebral tissues with qRT-PCR and western blot assays. We found that miR-124

mimics significantly decreased C/EBP-α levels compared with those of miR-124 inhibitors group (Fig.5D). Furthermore, microglia was transduced with miR-124 mimics or miR-124 control, and then treated with erythrocyte lysates. The similar negative regulation of miR-124 was also observed in vitro (Fig.5E).

MiR-124 enhanced microglia M2 polarization and attenuated inflammatory response via C/EBP-α

To identify the role of C/EBP-α in the miR-124 mediated inflammatory response inhibition, we attenuated C/EBP-α expression and detected the inflammation of microglia by siRNA assay. We found that C/EBP-α siRNA significantly decreased C/EBP-α mRNA and protein expression. However, scramble siRNA did not decrease C/EBP-α expression (Fig.6.A). In addition, inhibition of C/EBP-α significantly enhanced microglia M2 polarization. However, scramble siRNA had no similar effect (Fig.6.B). Inhibition of C/EBP-α significantly decreased the cerebral water content and improved neurological deficit (Fig.6.C). Additionally, inhibition of C/EBP-α significantly improved neuron viability in vitro (Fig.6.D). These data demonstrated that C/EBP-α contributed to miR-124 mediated inflammatory response inhibition.

Discussion

In the present study, we proved the effect of miR-124 on microglia M1/M2 polarization and brain inflammation after ICH. We addressed following issues: (1) MiR-124 expression level in vivo and in vitro after ICH; (2) The relationship between miR-124 and M1/M2 polarization in vivo and in vitro after ICH; (3) The regulation of miR-124 on inflammatory damage

in vivo and in vitro after ICH; (4) The regulation of miR-124 on the target C/EBP-α expression and the specific mechanism in vivo and in vitro after ICH.

The ICH hematoma surrounding tissue edema and secondary neural cell damage are the most important factors to influence the prognosis of patients. So exploring the pathophysiology of ICH surrounding tissue is becoming a hot spot of current research[26-28]. Accumulating evidence has shown that microglia plays an important role in the central nervous system[29-31]. In brain injury, cerebral ischemia, cerebral hemorrhage, and pathological conditions, such as the central nervous system infection, microglia can activate, proliferate, and express signaling molecules and cytokines to induce secondary brain damages[8,32,33]. Therefore, restrain the excessive activation of microglia and reducing the cytokine secretion of neurotoxicity will become new ways of ICH treatment.

Microglia secretes nerve toxicity factors and nutrition factors, and shows the dual role of proinflammatory and anti-inflammatory, characterized by M1 and M2 polarization state[34-36]. M1 microglia produces high levels of oxide metabolites and proinflammatory factor, such as IL-6, TNF-α, etc. Its effect is to eliminate the invasion of pathogenic microorganisms and cancer cell, but also lead to the normal cell and tissue damage. M2 microglia secretes high level of IL-10 and TGF-β. Its role is immune suppression, such as inhibition of M1 reaction, immune regulation, tissue repair and functional remodeling[37-39].

Numerous studies found that miRNA expression level altered in different microglia polarization. It was also reported that miRNAs regulated microglia polarization. For example, miR-155 and miR-146a are involved in M1

polarization and their expressions are promoted by IFN-γ or LPS stimulation[40]. Recent research demonstrated that miR-223 regulated the development of the M2 polarization in the adipose tissue[41]. In addition, miR-124 was regarded as the most abundant miRNAs in the cerebral and decreased in ischemic stroke[42]. However, the expression and the role of miR-124 on microglia polarization after ICH were less studied. In the previous study, we utilized a miRNA microarray to analyze miRNA expression profiles of microglia, and the results demonstrated that miR-124 levels were much lower compared with other miRNAs in microglia treated with erythrocyte lysates. Therefore, miR-124 was chosen to study in the further experiment.

Firstly, we utilized experimental ICH model and erythrocyte lysates-treated microglia model to measure miR-124 levels. We fount that level of miR-124 in ICH group was much lower than that in control group. Theses data demonstrated that ICH downregulated miR-124 expression in vivo and in vitro. Secondly, to further investigate the role of miR-124 on microglia M1/M2 polarization, we analyzed ICH induced M1/M2 markers in vivo and in vitro. ICH was done in the caudate nucleus, then miR-124 mimics or inhibitors was injected into the ventricle. After 3 days, the tissue of the perihematoma area was collected and investigated. We found that miR-124 mimics significantly decreased of M1 marker levels, while miR-124 inhibitors significantly increased M1 marker. Theses data demonstrated that miR-124 attenuated M1 marker expressions and promoted M2 marker expressions in vivo and in vitro. In addition, we detected the contribution of miR-124 to inflammatory injury in ICH. We measured water content and neurological injury in ICH mice and microglia toxicity to neuron. We found that miR-124 attenuated inflammatory injury and microglia

toxicity to neuron in vivo and in vitro. Furthermore, we also found that miR-124 significantly attenuated neuron apoptosis cells via Bcl-2/Bcl-xl pathway in vivo and in vitro.

C/EBP-α is one of the C/EBP transcription factor family members, which comprises six members (α-ζ)[23,43,44]. C/EBP proteins are widely expressed and regulate enormous cellular and physiological processes, including energy metabolism, immunity, inflammation, hematopoiesis, and adipogenesis[45,46]. C/EBP-α is highly expressed in early myeloid progenitors and may regulate monocyte and macrophage development[47]. Having found miR-124 attenuated microgila activation, we further investigated the mechanism underlying this effect. Using the TargetScan algorithm, we utilized in silico analysis of mRNA targets predicted for miR-124. C/EBP-α, a master transcription factor involved in differentiation of myeloid cells, was predicted as a putative target, with one conserved miR-124 binding sites within its 3′ untranslated region. We identified miR-124 reduced C/EBP-α expression in microglia. As C/EBP-α is one of the M1 polarization transcription factors, we hypothesized that miR-124 downregulated inflammation through inhibition of C/EBP-α. To test this hypothesis, we used RNAi strategy to reduce levels of C/EBP-α protein, which resulted in reduced expression of IL-6, IL-1β, and TNF-α levels. These data suggested that miR-124 attenated microglia activation by direct inhibition of C/EBP-α. However, miRNA can have hundreds of targets and a miRNA exerts its regulatory capacity by targeting several transcripts in a cell. C/EBP-α is one of many potential targets of miR-124 and downregulation of C/EPB-α might not the specific mechanism.

Taken together, our findings demonstrate that miR-124 has a key role in inhibiting microglia activation and promoting microglia M2 polarization in

ICH. In addition, in vivo administration of miR-124 attenuates inflammatory injury provides promising therapeutical strategy in ICH.

Acknowledgements

This study was supported by a research grant from the NSFC No.81560217.

Reference

[1] Bonsack Ft, Alleyne CH, Jr., Sukumari-Ramesh S. Augmented expression of TSPO after intracerebral hemorrhage: a role in inflammation? Journal of neuroinflammation;2016;13:151.

[2] Zheng H, Chen C, Zhang J, Hu Z. Mechanism and Therapy of Brain Edema after Intracerebral Hemorrhage. Cerebrovascular diseases (Basel, Switzerland); 2016;42:155-169.

[3] Hsieh JT, Ang BT, Ng YP, Allen JC, King NK. Comparison of Gender Differences in Intracerebral Hemorrhage in a Multi-Ethnic Asian Population. PloS one; 2016;11:e0152945.

[4] Tao C, Zhang R, Hu X, Song L, Wang C, Gao F, You C. A Novel Brainstem Hemorrhage Model by Autologous Blood Infusion in Rat: White Matter Injury, Magnetic Resonance Imaging, and Neurobehavioral Features. J Stroke Cerebrovasc Dis; 2016;25:1102-1109.

[5] Guo Z, Sun L, Dong Q, Liu C, Zhou R, Gong S, Wang G. A case report of successful conservative treatment for huge acute traumatic intracerebral hematoma. Medicine; 2015;94:e656.

[6] Wei G, Lu XC, Shear DA, Yang X, Tortella FC. Neuroprotection of Selective Brain Cooling After Penetrating Ballistic-like Brain Injury in Rats. Therapeutic hypothermia and temperature management; 2011;1:33-42.

[7] Zheng J, Liu Z, Li W, Tang J, Zhang D, Tang X. Lithium posttreatment confers neuroprotection through glycogen synthase kinase-3beta inhibition in intracerebral hemorrhage rats. Journal of neurosurgery: 2015;1-9.

[8] Zhou K, Zhong Q, Wang YC, Xiong XY, Meng ZY, Zhao T, Zhu WY, Liao MF, Wu LR, Yang YR, Liu J, Duan CM, Li J, Gong QW, Liu L, Yang MH, Xiong A, Wang J, Yang QW. Regulatory T cells ameliorate intracerebral hemorrhage-induced inflammatory injury by modulating microglia/macrophage polarization through the IL-10/GSK3beta/PTEN axis. J Cereb Blood Flow Metab. 2016; [Epub ahead of print]

[9] Weng X, Tan Y, Chu X, Wu XF, Liu R, Tian Y, Li L, Guo F, Ouyang Q, Li L. N-methyl-D-aspartic acid receptor 1 (NMDAR1) aggravates secondary inflammatory damage induced by hemin-NLRP3 pathway after intracerebral hemorrhage. Chinese journal of traumatology = Zhonghua chuang shang za zhi; 2015;18:254-258.

[10] Francos-Quijorna I, Amo-Aparicio J, Martinez-Muriana A, Lopez-Vales R. IL-4 drives microglia and macrophages toward a phenotype conducive for tissue repair and functional recovery after spinal cord injury. Glia; 2016;64:2079-2092.

[11] Lee JH, Wei ZZ, Cao W, Won S, Gu X, Winter M, Dix TA, Wei L, Yu SP. Regulation of therapeutic hypothermia on inflammatory cytokines, microglia polarization, migration and functional recovery after ischemic stroke in mice. Neurobiology of disease; 2016;96:248-260.

[12] Shi H, Zheng K, Su Z, Su H, Zhong M, He X, Zhou C, Chen H, Xiong Q, Zhang Y. Sinomenine enhances microglia M2 polarization and attenuates inflammatory injury in intracerebral hemorrhage. Journal of neuroimmunology; 2016;299:28-34.

[13] Xu X, Gao Y, Wen L, Zhai Z, Zhang S, Shan F, Feng J. Methionine enkephalin regulates microglia polarization and function. International immunopharmacology; 2016;40:90-97.

[14] Plastira I, Bernhart E, Goeritzer M, Reicher H, Kumble VB, Kogelnik N, Wintersperger A, Hammer A, Schlager S, Jandl K, Heinemann A, Kratky D, Malle E, Sattler W.

1-Oleyl-lysophosphatidic acid (LPA) promotes polarization of BV-2 and primary murine microglia towards an M1-like phenotype. Journal of neuroinflammation; 2016;13:205.

[15] Hamzei Taj S, Kho W, Aswendt M, Collmann FM, Green C, Adamczak J, Tennstaedt A, Hoehn M. Dynamic Modulation of Microglia/Macrophage Polarization by miR-124 after Focal Cerebral Ischemia. J Neuroimmune Pharmacol; 2016;11:733-748.

[16] Haug BH, Hald OH, Utnes P, Roth SA, Lokke C, Flaegstad T, Einvik C. Exosome-like Extracellular Vesicles from MYCN-amplified Neuroblastoma Cells Contain Oncogenic miRNAs. Anticancer research; 2015;35:2521-2530.

[17] Guescini M, Canonico B, Lucertini F, Maggio S, Annibalini G, Barbieri E, Luchetti F, Papa S, Stocchi V. Muscle Releases Alpha-Sarcoglycan Positive Extracellular Vesicles Carrying miRNAs in the Bloodstream. PloS one; 2015;10:e0125094.

[18] Xue F, Shen R, Chen X. Analysis of gene profiles in glioma cells identifies potential genes, miRNAs, and target sites of migratory cells. Tumori; 2015;101:542-548.

[19] Veremeyko T, Siddiqui S, Sotnikov I, Yung A, Ponomarev ED. IL-4/IL-13-dependent and independent expression of miR-124 and its contribution to M2 phenotype of monocytic cells in normal conditions and during allergic inflammation. PloS one; 2013;8:e81774.

[20] Moore CS, Rao VT, Durafourt BA, Bedell BJ, Ludwin SK, Bar-Or A, Antel JP. miR-155 as a multiple sclerosis-relevant regulator of myeloid cell polarization. Annals of neurology; 2013;74:709-720.

[21] Ponomarev ED, Veremeyko T, Weiner HL. MicroRNAs are universal regulators of differentiation, activation, and polarization of microglia and macrophages in normal and diseased CNS. Glia; 2013;61:91-103.

[22] Willemen HL, Huo XJ, Mao-Ying QL, Zijlstra J, Heijnen CJ, Kavelaars A. MicroRNA-124 as a novel treatment for persistent hyperalgesia. Journal of neuroinflammation; 2012;9:143.

[23] Ponomarev ED, Veremeyko T, Barteneva N, Krichevsky AM, Weiner HL. MicroRNA-124 promotes microglia quiescence and suppresses EAE by deactivating macrophages via the C/EBP-alpha-PU.1 pathway. Nature medicine; 2011;17:64-70.

[24] Yuan B, Fu F, Huang S, Lin C, Yang G, Ma K, Shi H, Yang Z. C5a/C5aR Pathway Plays a Vital Role in Brain Inflammatory Injury via Initiating Fgl-2 in Intracerebral Hemorrhage. Molecular neurobiology. 2016; **12**, 236-245

[25] Yu A, Duan H, Zhang T, Pan Y, Kou Z, Zhang X, Lu Y, Wang S, Yang Z. IL-17A promotes microglial activation and neuroinflammation in mouse models of intracerebral haemorrhage. Molecular immunology; 2016;73:151-157.

[26] Wu H, Wu T, Han X, Wan J, Jiang C, Chen W, Lu H, Yang Q, Wang J. Cerebroprotection by the neuronal PGE2 receptor EP2 after intracerebral hemorrhage in middle-aged mice. J Cereb Blood Flow Metab. 2016; **10**, 56-64

[27] Zhang Y, Chen Y, Wu J, Manaenko A, Yang P, Tang J, Fu W, Zhang JH. Activation of Dopamine D2 Receptor Suppresses Neuroinflammation Through alphaB-Crystalline by Inhibition of NF-kappaB Nuclear Translocation in Experimental ICH Mice Model. Stroke; a journal of cerebral circulation; 2015;46:2637-2646.

[28] Leclerc JL, Ahmad AS, Singh N, Soshnik-Schierling L, Greene E, Dang A, Dore S. Intracerebral hemorrhage outcomes following selective blockade or stimulation of the PGE2 EP1 receptor. BMC neuroscience; 2015;16:48.

[29] Piotrowska A, Kwiatkowski K, Rojewska E, Makuch W, Mika J. Maraviroc reduces neuropathic pain through polarization of microglia and astroglia - Evidence from in vivo and in vitro studies. Neuropharmacology; 2016;108:207-219.

[30] Weng L, Wu Z, Zheng W, Meng H, Han L, Wang S, Yuan Z, Xu Y. Malibatol A enhances alternative activation of microglia by inhibiting phosphorylation of Mammalian Ste20-like kinase1 in OGD-BV-2 cells. Neurological research; 2016;38:342-348.

[31] Hernandez-Rabaza V, Cabrera-Pastor A, Taoro-Gonzalez L, Gonzalez-Usano A, Agusti A, Balzano T, Llansola M, Felipo V. Neuroinflammation increases GABAergic tone and impairs cognitive and motor function in hyperammonemia by increasing GAT-3 membrane expression. Reversal by sulforaphane by promoting M2 polarization of microglia. Journal of neuroinflammation; 2016;13:83.

[32] Wan S, Cheng Y, Jin H, Guo D, Hua Y, Keep RF, Xi G. Microglia Activation and Polarization After Intracerebral Hemorrhage in Mice: the Role of Protease-Activated Receptor-1. Translational

stroke research; 2016;7:478-487.
[33] Xiong XY, Liu L, Yang QW. Functions and mechanisms of microglia/macrophages in neuroinflammation and neurogenesis after stroke. Progress in neurobiology; 2016;142:23-44.
[34] Ransohoff RM. A polarizing question: do M1 and M2 microglia exist? Nature neuroscience; 2016;19:987-991.
[35] Wang Y, Duan W, Wang W, Di W, Liu Y, Liu Y, Li Z, Hu H, Lin H, Cui C, Li D, Dong H, Li C. scAAV9-VEGF prolongs the survival of transgenic ALS mice by promoting activation of M2 microglia and the PI3K/Akt pathway. Brain research; 2016;1648:1-10.
[36] Li D, Wang C, Yao Y, Chen L, Liu G, Zhang R, Liu Q, Shi FD, Hao J. mTORC1 pathway disruption ameliorates brain inflammation following stroke via a shift in microglia phenotype from M1 type to M2 type. Faseb J; 2016;30:3388-3399.
[37] Meng HL, Li XX, Chen YT, Yu LJ, Zhang H, Lao JM, Zhang X, Xu Y. Neuronal Soluble Fas Ligand Drives M1-Microglia Polarization after Cerebral Ischemia. CNS neuroscience & therapeutics; 2016;22:771-781.
[38] Arroba AI, Alcalde-Estevez E, Garcia-Ramirez M, Cazzoni D, de la Villa P, Sanchez-Fernandez EM, Mellet CO, Garcia Fernandez JM, Hernandez C, Simo R, Valverde AM. Modulation of microglia polarization dynamics during diabetic retinopathy in db/db mice. Biochimica et biophysica acta; 2016;1862:1663-1674.
[39] Esslinger M, Wachholz S, Manitz MP, Plumper J, Sommer R, Juckel G, Friebe A. Schizophrenia associated sensory gating deficits develop after adolescent microglia activation. Brain, behavior, and immunity; 2016;58:99-106.
[40] Pareek S, Roy S, Kumari B, Jain P, Banerjee A, Vrati S. MiR-155 induction in microglial cells suppresses Japanese encephalitis virus replication and negatively modulates innate immune responses. Journal of neuroinflammation; 2014;11:97.
[41] Zhuang G, Meng C, Guo X, Cheruku PS, Shi L, Xu H, Li H, Wang G, Evans AR, Safe S, Wu C, Zhou B. A novel regulator of macrophage activation: miR-223 in obesity-associated adipose tissue inflammation. Circulation; 2012;125:2892-2903.
[42] Svahn AJ, Giacomotto J, Graeber MB, Rinkwitz S, Becker TS. miR-124 Contributes to the functional maturity of microglia. Developmental neurobiology; 2016;76:507-518.
[43] Rao KN, Smuda C, Gregory GD, Min B, Brown MA. Ikaros limits basophil development by suppressing C/EBP-alpha expression. Blood; 2013;122:2572-2581.
[44] Regalo G, Resende C, Wen X, Gomes B, Duraes C, Seruca R, Carneiro F, Machado JC. C/EBP alpha expression is associated with homeostasis of the gastric epithelium and with gastric carcinogenesis. Laboratory investigation; a journal of technical methods and pathology; 2010;90:1132-1139.
[45] Chase KA, Rosen C, Gin H, Bjorkquist O, Feiner B, Marvin R, Conrin S, Sharma RP. Metabolic and inflammatory genes in schizophrenia. Psychiatry research; 2014;225:208-211.
[46] Roth M, Black JL. An imbalance in C/EBPs and increased mitochondrial activity in asthmatic airway smooth muscle cells: novel targets in asthma therapy? British journal of pharmacology 2009;157:334-341.
[47] Chen W, Zhu G, Hao L, Wu M, Ci H, Li YP. C/EBPalpha regulates osteoclast lineage commitment. Proceedings of the National Academy of Sciences of the United States of America; 2013;110:7294-7299.

Figure legends

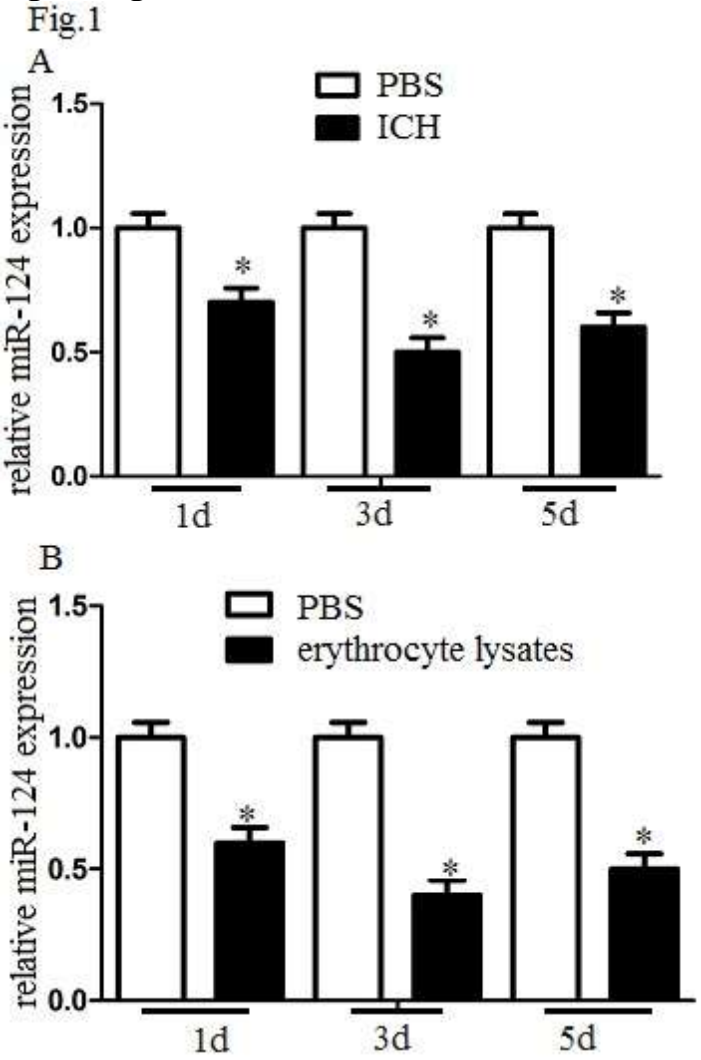

Fig.1. MiR-124 expression was downregulated in perihematoma tissue of ICH mice and erythrocyte lysates-treated microglia

(A) Mice were deeply anaesthetized and transcardially at 1, 3, or 5 days after ICH. The brains were removed and post-fixed. The perihaematomal region of cerebral tissue was collected, and the tissue lysates were further analyzed for miR-124 mRNA expression by quantitative RT-PCR. (B) Microglia (1×10^5) was stimulated with 10 μl PBS or erythrocyte lysates for 1, 3, or 5 days. After then, the cell lysates were further analyzed for miR-124 mRNA expression by quantitative RT-PCR. Experiments performed in triplicate

showed consistent results. Data are presented as the mean±SD of three independent experiments. *P < 0.05

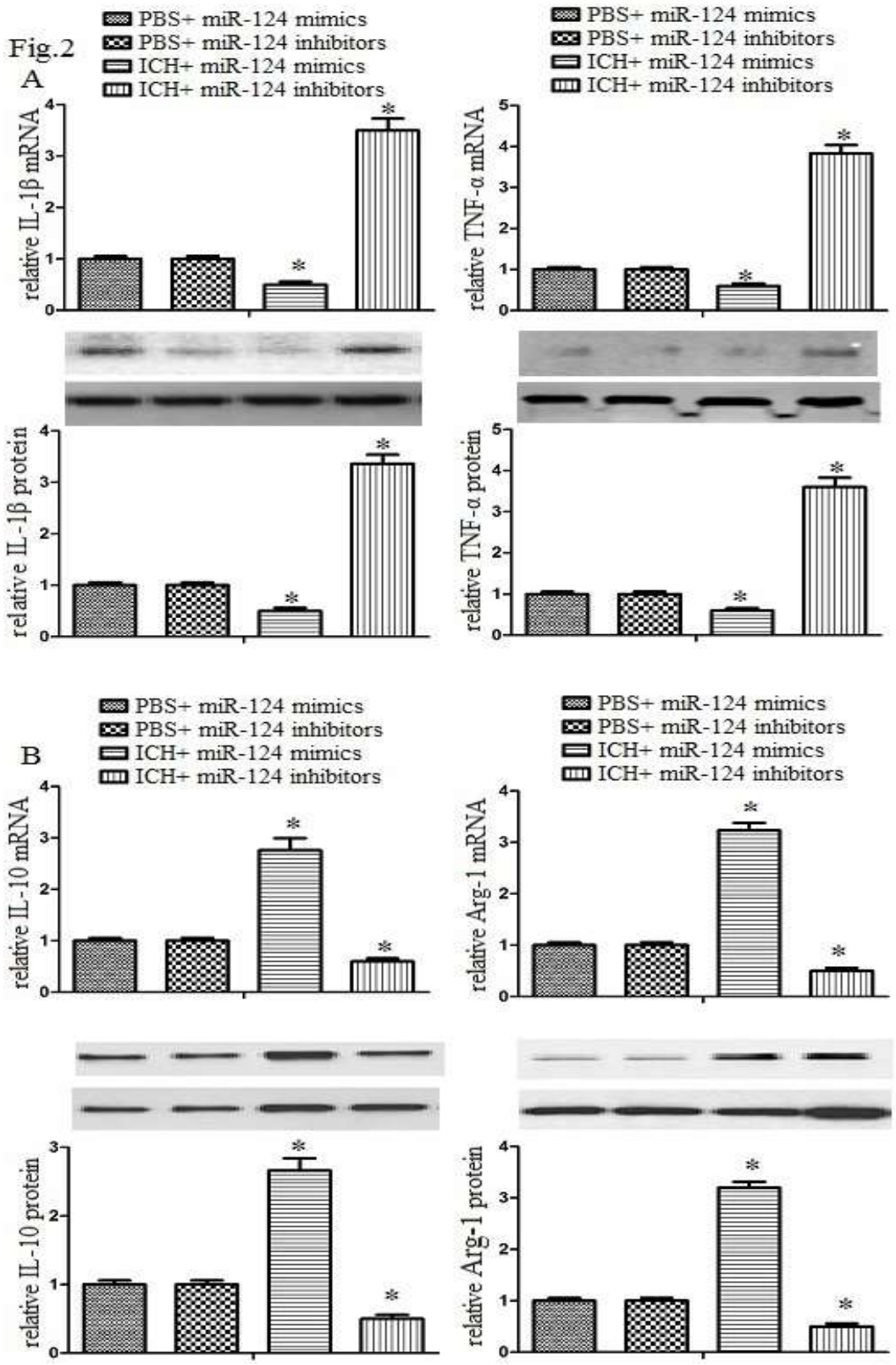

Fig.2. MiR-124 enhanced microglia M2 polarization in vivo

(A)Intracerebroventricular injection of miR-124 mimics or inhibitors was administered 10 min after ICH. Mice were deeply anaesthetized and transcardially at 3 days after ICH. The brains were removed and post-fixed. The perihaematomal region of cerebral tissue was collected, and the tissue lysates were further analyzed for miR-124 mRNA expression by qRT-PCR. (B) M1/M2 markers of the tissue lysates were further analyzed by qRT-PCR and western blot assays. (C) M2 markers of the tissues were analyzed by immunofluorescence. Experiments performed in triplicate showed consistent results. Data are presented as the mean±SD of three independent experiments. *$P < 0.05$

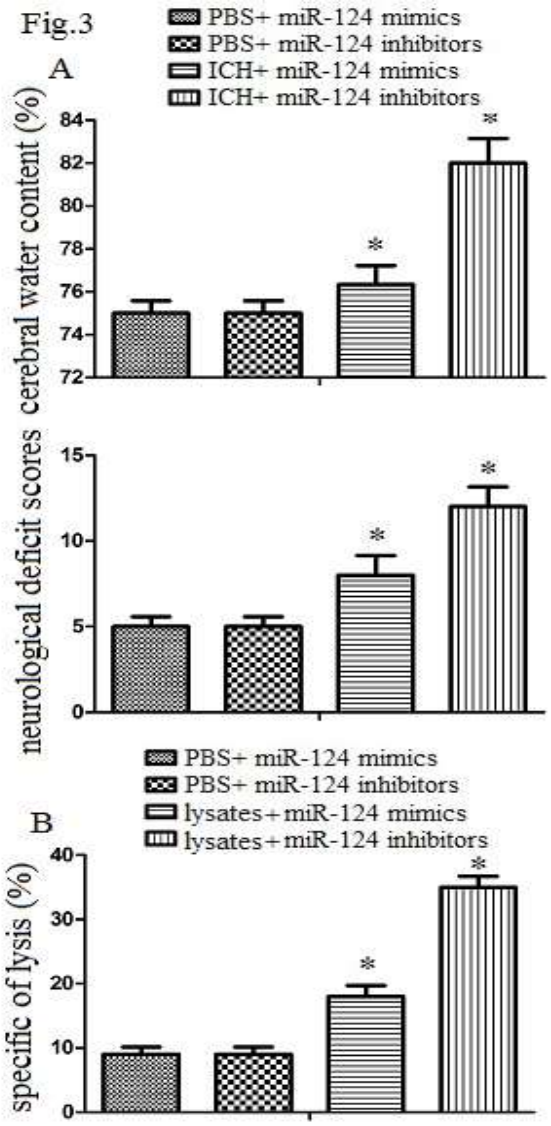

Fig.3. MiR-124 attenuated inflammatory damage in vivo and in vitro

(A) Intracerebroventricular injection of miR-124 mimics or inhibitors was administered 10 min after ICH. After 3 days of ICH, the cerebral water content of mice (n = 5) was also analyzed. (B) In addition, the neurological deficit tests were performed by behavioral measurement, including a composite of motor, sensory, reflex, and balance tests. (C) Microglia was transduced with miR-124 mimics or inhibitors, and then was treated with PBS or erythrocyte lysates for 3 days. To detect the microglia cytotoxicity to neuron, we cocultured the neuron with a mixture of microglia conditioned

medium, and the cytotoxic activity of microglia was analyzed by a 6 h lactate dehydrogenase release assay. Experiments were performed in quadruplet and the percentage of lysis was determined by OD490 measurement as described in the manufacturer's instructions. Experiments performed in triplicate showed consistent results. Data are presented as the mean±SD of three independent experiments. *$P < 0.05$

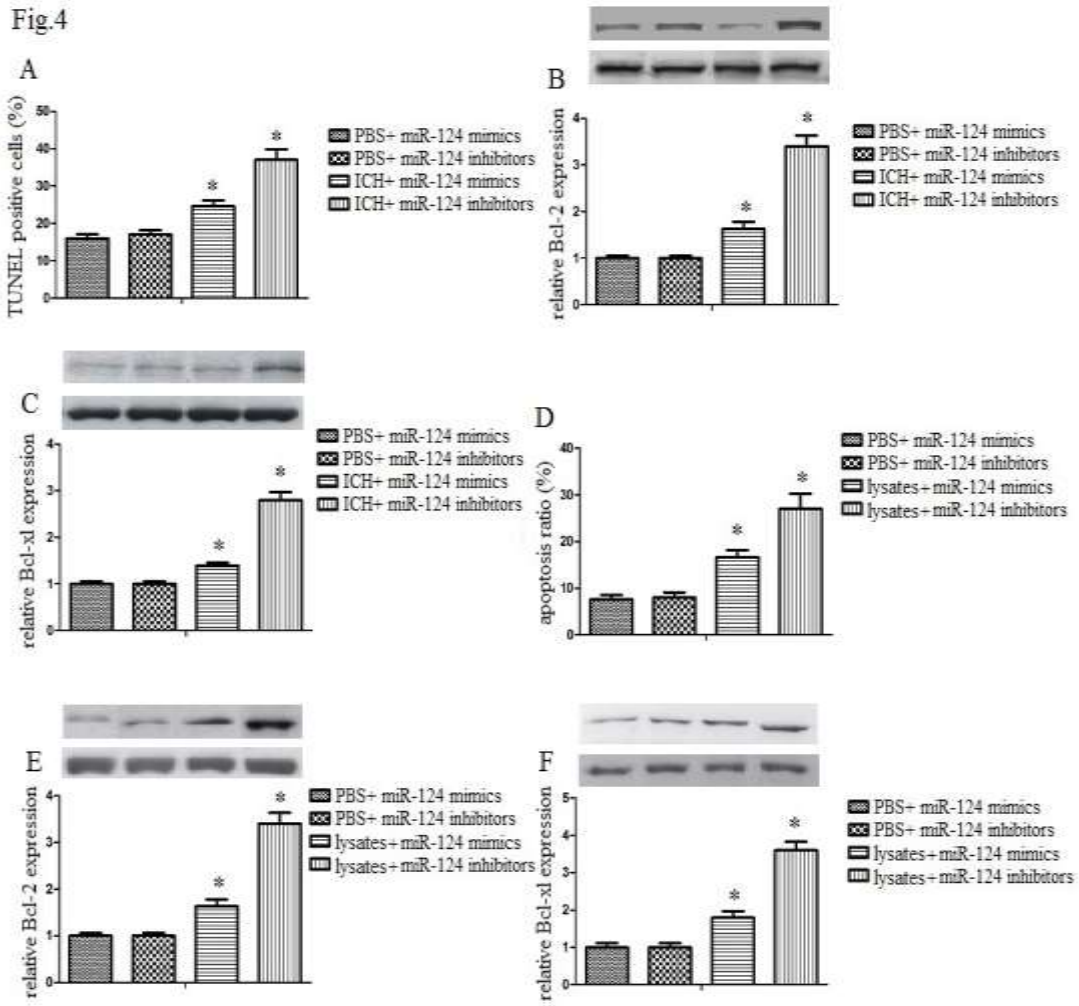

Fig.4. MiR-124 attenuated neuron apoptosis via Bcl-2/Bcl-xl pathway

(A) Intracerebroventricular injection of miR-124 mimics or inhibitors was administered 10 min after ICH. Mice were deeply anaesthetized and transcardially at 3 days after ICH. The brains were removed and post-fixed. The perihaematomal region of cerebral tissue was collected, TUNEL staining was performed. The percentage of TUNEL positive cells were calculated using the formula red/blue×100%. The number of positive cells in each quadrant was counted. (B-C) The perihaematomal region of cerebral tissue was collected, and Bcl-2 and Bcl-xl expression were examined by western blot assays. (D) Microglia was transduced with miR-124 mimics or

inhibitors, and then was treated with PBS or erythrocyte lysates for 3 days. After then, neuron was treated with conditioned medium from treated microglia. After 48 h, neuron apoptosis ratio was detected by flow cytometry. Apoptosis cells were determined by Annexin V positive and propidium iodide (PI) negative cells. (E-F) The cell lysates were collected, Bcl-2 and Bcl-xl expression were examined by western blot assays. Experiments performed in triplicate showed consistent results. Data are presented as the mean±SD of three independent experiments. *$P < 0.05$

Fig.5

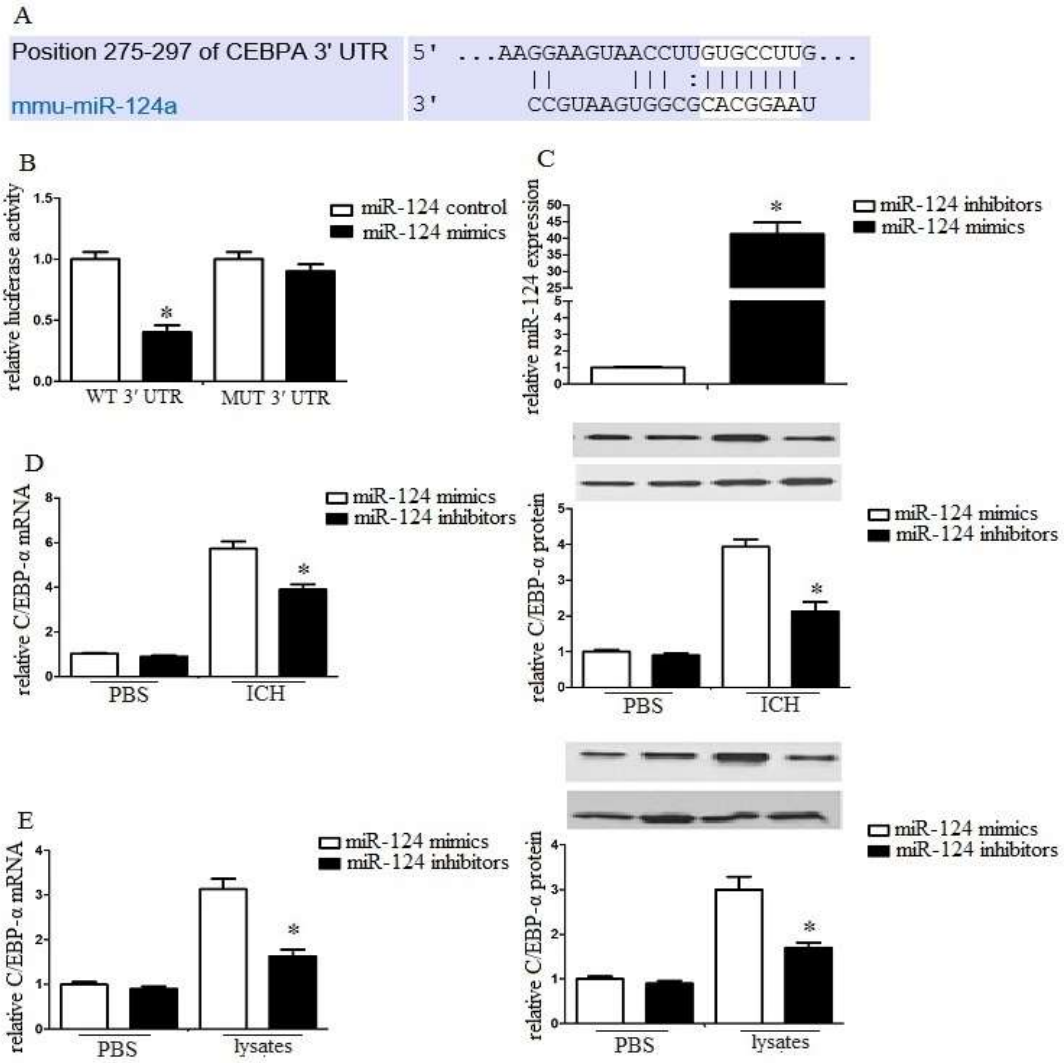

Fig.5. MiR-124 regulated C/EBP-α expression in vivo and in vitro

(A) C/EBP-α is a direct target of miR-124 in microglia. C/EBP-α 3′ UTR fragment containing wild-type or mutant miR-124-binding sites was cloned downstream of the luciferase reporter gene. The region of the C/EBP-α mRNA 3′ UTR predicted to be targeted by miR-124 as indicated. (B) Luciferase activity assays using reporters with wild-type or mutant C/EBP-α 3′ UTRs were performed after cotransfection with miR-124 mimics or control in microglia. The luciferase activity of the control transfection in each experiment was used to normalize the data, and the luciferase activity

of the control transfection was set equal to 1. (C) Microglia was transfected with miR-124 mimics or inhibitors. After 24 h, cells were harvested, and miR-124 expression was evaluated by qRT-PCR. (D) Intracerebroventricular injection of miR-124 mimics or inhibitors was administered 10 min after ICH. Mice were deeply anaesthetized and transcardially at 3 days after ICH. The brains were removed and post-fixed. The C/EBP-α expression in the perihaematomal region of cerebral tissues was analyzed by qRT-PCR and western blot assays. (E) Microglia was transfected with miR-124 mimics or inhibitors, and then was treated with PBS or erythrocyte lysates for 3 days. After then, neuron was treated with conditioned medium from treated microglia. After 48 h, The C/EBP-α expression in the perihaematomal region of cerebral tissues was analyzed by qRT-PCR and western blot assays. Experiments performed in triplicate showed consistent results. Data are presented as the mean±SD of three independent experiments. *$P < 0.05$

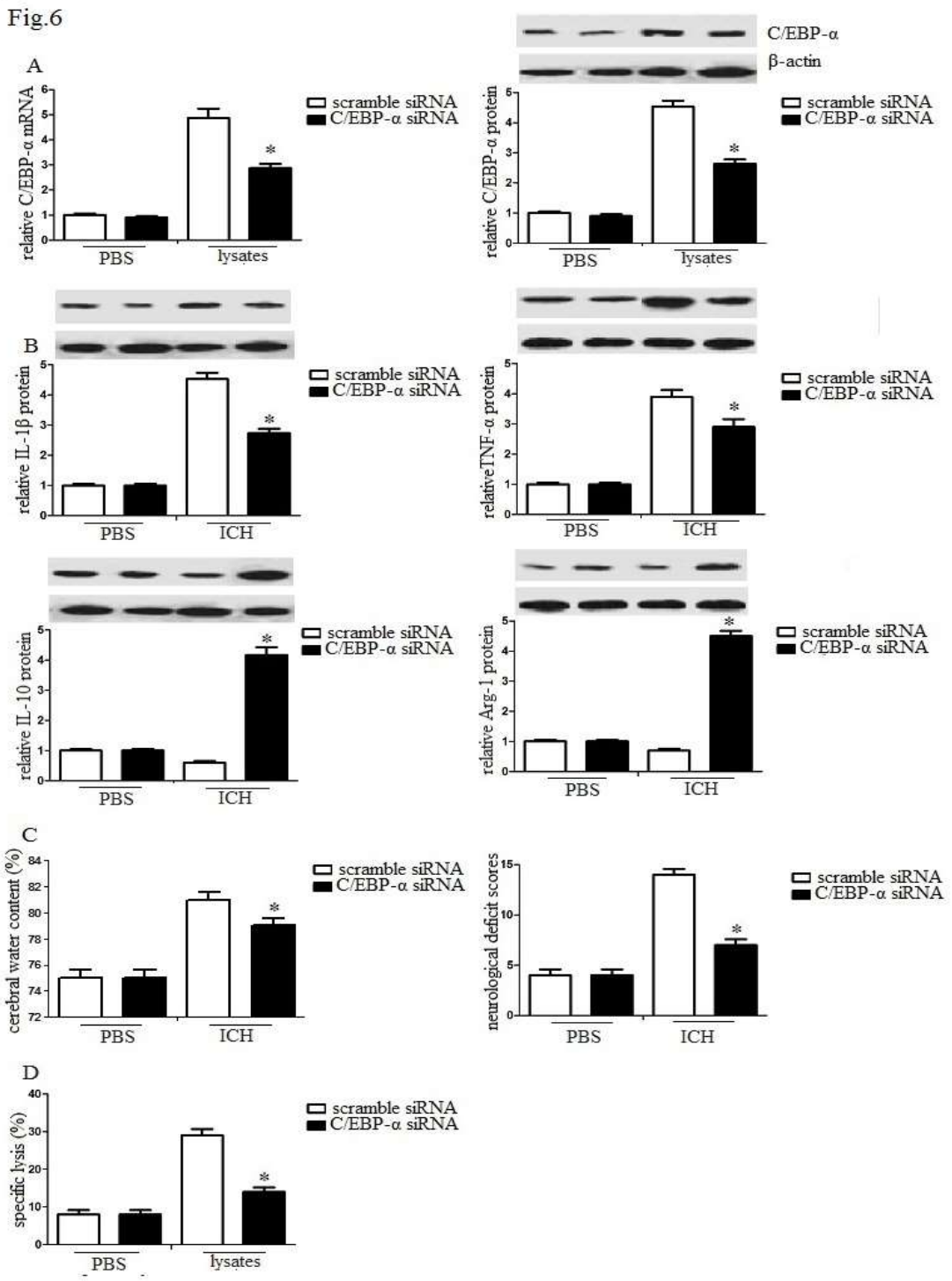

Fig.6.MiR-124 enhanced microglia M2 polarization and attenuated inflammatory response via C/EBP-α

(A) Detection of the inhibition efficiency of siRNAs against C/EBP-α.

Microglia was transfected with scramble siRNA or C/EBP-α siRNA and then exposed to erythrocyte lysates. After 48 h, C/EBP-α expression was analyzed by qRT-PCR and western blot assays. (B) Intracerebroventricular injection of scramble siRNA or C/EBP-α siRNA was administered 10 min after ICH. Mice were deeply anaesthetized and transcardially at 3 days after ICH. The perihaematomal region of cerebral tissue was collected, and M1/M2 markers of the tissue lysates were further analyzed by western blot assays. (C)After 3 days of ICH, the cerebral water content of mice (n=10) was also analyzed. In addition, the neurological deficit tests were performed by behavioral measurement. (D) Microglia was transfected with scramble siRNA or C/EBP-α siRNA, and then was treated with PBS or erythrocyte lysates for 3 days. After then, neuron was treated with conditioned medium from treated microglia. After 48 h, MTT reagent was added and the neuron viability was assessed. Experiments performed in triplicate showed consistent results. Data are presented as the mean±SD of three independent experiments. *$P < 0.05$